Quantifying factors affecting contributions of roadway exhaust and non-exhaust emissions to ambient $PM_{10–2.5}$ and $PM_{2.5–0.2}$ particles

Matthaios, Vasileios N.; Lawrence, Joy; Martins, Marco A.G.; Ferguson, Stephen T.; Wolfson, Jack M.; Harrison, Roy M.; Koutrakis, Petros

DOI:
10.1016/j.scitotenv.2022.155368

Quantifying factors affecting contributions of roadway exhaust and non-exhaust emissions to ambient coarse and fine particles

Vasileios N. Matthaios[1,2*], Joy Lawrence[1], Marco A. G. Martins[1], Stephen T. Ferguson[1], Jack M. Wolfson[1], Roy M. Harrison[2,3], Petros Koutrakis[1]

[1] Department of Environmental Health, Harvard T.H. Chan School of Public Health, Boston, MA, USA

[2] School of Geography Earth and Environmental Science, University of Birmingham, Birmingham, UK

[3] Department of Environmental Sciences / Center of Excellence in Environmental Studies, King Abdulaziz University, Jeddah, Saudi Arabia

*corresponding author: Harvard T.H. Chan School of Public Health, Department of Environmental Health, 401 Park Drive, Boston, MA 02215

Email: vmatthaios@hsph.harvard.edu

Abstract

Traffic-related particulate matter (PM) plays an important role in urban air pollution. However, sources of urban pollution are difficult to distinguish. This study utilises a mobile particle concentrator platform and statistical tools to investigate factors affecting roadway ambient coarse particle ($PM_{10-2.5}$) and fine particle ($PM_{2.5-0.2}$) concentrations in greater Boston, USA. Positive matrix factorization (PMF) identified six $PM_{10-2.5}$ sources (exhaust, road salt, brake wear, regional pollution, road dust resuspension and tyre-road abrasion) and seven fine particle sources. The seven $PM_{2.5-0.2}$ sources include the six $PM_{10-2.5}$ sources and a source rich in Cr and Ni. Non- exhaust traffic-related sources together accounted for 65.6% and 29.1% of the $PM_{10-2.5}$ and $PM_{2.5-0.2}$ mass, respectively. While the respective contributions of exhaust sources were 10.4% and 20.7%. The biggest non-exhaust contributor in the $PM_{10-2.5}$ was road dust resuspension, accounting for 29.6%, while for the $PM_{2.5-0.2}$, the biggest non-exhaust source was road-tyre abrasion, accounting for 12.3%. We used stepwise general additive models (sGAMs) and found statistically significant ($p < 0.05$) effects of temperature, number of vehicles and rush hour periods on exhaust, brake wear, road dust resuspension and road-tyre abrasion with relative importance between 19.1 - 71.5%, 12.5 – 42.1% and 4.4 – 42.2% of the sGAM model's explained variability. Meteorological variables of wind speed and relative humidity were significantly associated with both coarse and fine road dust resuspension and had a combined relative importance of 38% and 48%. The quantifying results of the factors that influence traffic-related sources can offer key insights to policies aiming to improve near-road air quality.

Keywords: particulate matter, source apportionment, non-exhaust, road traffic, air quality

1 Introduction

Road traffic is widely recognised as a significant contributor to urban particulate matter (PM). Exposure to traffic-related PM has been associated with various human adverse health effects, including asthma onset and exacerbation (Carlsten et al., 2011), lung growth deficits (Gauderman et al., 2007), increased blood pressure, decreased heart rate variability (Zanobetti et al., 2010), coronary heart disease hospitalizations and mortality (Gan et al., 2011), and low birth weight (Wilhelm et al., 2012).

In epidemiological studies, residential road proximity is often used as a proxy for traffic-related PM exposure. The relationship between road dust, ambient roadway coarse, and fine concentrations, mass, and distance from the road was examined in previous studies and showed significant reductions in $PM_{10-2.5}$ and $PM_{2.5-0.2}$ with increasing distance, by up to 30% and 4%, respectively, while elements linked to traffic related sources (*i.e.,* Cu, Ba, Zr) exhibited greater reductions, between 20-60% (Silva et al., 2021; Huang et al., 2020). Distance from the road also affects indoor concentrations, where houses within the first 15 m compared to those located at 1.8 km from the road were also found to have 1.3 and 2.1 times greater $PM_{2.5}$ and BC concentrations, respectively, while levels of Mn and Mo also differ considerably, by factors of 10.9 and 6.5, respectively (Huang et al., 2018).

Distance to roadway has been used as a surrogate for traffic-related PM when analysing associations with health effects. However, this surrogate provides no insight into which of the specific sources/origins or components of traffic-related PM are more toxic. Traffic-related PM is a complex mixture originating from both direct vehicular tailpipe and non-tailpipe emissions and non-direct vehicle emissions such as road dust resuspension. Exhaust emissions include elemental and organic carbon and various trace elements associated with incomplete combustion of fuel and oil additives. Non-exhaust emissions include particles mainly from brake wear, tyre wear, engines, and abrasion between tyre and road surfaces. Road dust resuspension typically contains high concentrations of heavy metals originating from tailpipe and non-tailpipe emissions, as well as crustal material (soil and sand), road salt abrasion of road surfaces and vegetation debris (Harrison et al., 2012; Lawrence et al., 2021). In the USA, road dust resuspension (as % of all road transport emissions) is responsible for 65% and 79% of fine and coarse emissions, respectively (USEPA, 2019). As exhaust emissions of PM from road vehicles have gradually been reduced due to the new after-treatment technologies and stricter legislative limits (Harrison and Beddows 2017; Matthaios et al., 2019), non-exhaust emissions have become an increasing proportion of the total road emissions, and in many countries now exceed exhaust emissions (Amato et al., 2014a).

Sources of traffic-related PM are often identified using chemical tracers and receptor modelling techniques (Harrison et al., 2021). However, since different materials are used for brake pads and tyres from car manufacturers across the globe, non-exhaust PM profiles can be highly variable (Pant and Harrison, 2013). Also, both exhaust and non-exhaust PM emissions typically vary with different driving styles, fleet composition and road type variations, making source apportionment even more challenging. The electrification of vehicle fleets and new technologies such as regenerative braking may also change the source apportionment at roadside locations. In a recent review of non-exhaust emissions, Padoan and Amato (2018) reviewed 256 source apportionment studies and found that 71% of these showed only road dust contributions. Only 8% and 9% of these studies could show brake and tyre wear contributions, respectively, while 12% of them reported a generic source of non-exhaust emissions. Aiming at improving our understanding of near-road PM sources and the factors affecting them, this study utilises a mobile particle concentrator platform to investigate the coarse and fine roadside PM sources in 90 different road locations in the greater Boston Massachusetts area. The study implements source apportionment and regression modelling techniques to identify key controllable factors that affect roadside PM sources as well as to quantify the joint and individual effects of meteorological parameters and road characteristics.

2 Methods

2.1 Roadway ambient coarse and fine PM sampling and analysis

The experimental campaign was conducted from June 2018 to December 2019 in the Greater Boston, USA metropolitan area. Roadway ambient coarse ($PM_{10-2.5}$) and fine ($PM_{2.5-0.2}$) PM fractions were sampled at different distances from major roadways. On each sampling day, ambient PM samples were collected at three distances from the road: roadside (0–25 m), intermediate distance (50–100 m), and local roadside background (> 250 m). Major roadways sampled included multi-lane divided state and interstate highways (with or without limited access via onramps and exit ramps) and busy state secondary and connecting roads. Background and intermediate samples were collected the same day at locations on adjacent roadways within the target distances from the roadside site and were almost entirely on residential roads. Overall 90 roadway location measurements were made, with 69 (23 x 3 different distance) roadway locations sampled once and 21 roads (7 x 3 different distance) sampled twice, in different seasons. 90 coarse and 90 fine samples were taken, while the sample sites were carefully selected in order to avoid areas with non-traffic-related emission sources nearby. Figure 1 shows the locations of the sampling sites. For sampling, a modified Harvard Ambient Fine Particle Concentrator (HAFPC), originally a 5,500 litres per minute (LPM) three stage fine particle concentrator that was described in detail in previous studies (Lawrence et al. 2004; Sioutas et al. 1997) was used in a mobile platform, described in detail elsewhere (Martins et al., 2021). Briefly, the modified system used two parallel two-stage concentrators each with intake flowrate of 1,100 LPM. Concentrator outputs were combined, followed by collection of samples on Teflon and quartz fibre filters in parallel, with sample flows of 45 LPM for each. We analysed the Teflon filter for mass and elemental composition, and the quartz filters for elemental and organic carbon. Samples were collected for one hour; ambient concentrations were calculated using the concentrator enrichment factor as described elsewhere (Martins et al., 2021). The quartz filters were purchased pre-fired, packaged in petri dishes and wrapped in foil. After sampling, they were sealed in petri dishes, wrapped in foil and stored in plastic bags in a lab freezer prior to EC/OC analysis. The Teflon filters were conditioned in a temperature- and humidity-controlled room prior to weighing and sealed in plastic petri dishes before and after sample collection. Blanks were collected and analyzed for both quartz and Teflon filters but no correction was necessary because they were negligible.

Figure 1. Sampling locations of the mobile platform in greater Boston area

The PM concentrations were determined by gravimetric analysis and the collected samples were analysed for elemental composition by X-Ray Fluorescence (XRF) analysis. A microbalance (model MT-5, Mettler-Toledo, Columbus, Ohio) in a temperature and humidity-controlled room was used for gravimetric analysis. XRF was performed using a PANalytical Epsilon 5 spectrometer (Malvern PANalytical, Almelo, the Netherlands). Element detection limits and their uncertainties can be found in Martins et al., (2021). We further analysed each quartz filter sample for elemental carbon (EC) and organic carbon (OC) using thermal optical reflectance (TOR) (Moreira et al., 2021; Lawrence et al., 2021).

2.2 Positive Matrix Factorization (PMF)

PMF is a receptor model that uses a multivariate factor analysis based on weighted least square fits, and realistic error estimates to weight data values by enforcing non-negative constraints in the factor computational process. Here, the United States Environmental Protection Agency (USEPA) PMF 5.0 model was used (Norris et al., 2014) and we added an additional 10% uncertainty in the model runs to account for the uncertainty in the sampling methods (Martins et al., 2021). Since PMF is a weighted least-squares method, individual estimates of the uncertainty in each data value are necessary. The uncertainty input data matrix followed the approaches described by Norris et al. (2014) and Polissar et al. (1998) by including the measurement uncertainty of each sample element. The missing data and the data below the detection limit were replaced with the mean concentration of the corresponding species over the entire measurement matrix and they were accompanied by an uncertainty of 4 times the species-specific mean, as suggested in Norris et al. (2014). To acquire realistic source profiles and an optimum number of factors, multiple criteria were used including: 1) signal to noise ratio; 2) symmetric distribution of scaled residuals ($\pm 3\sigma$); 3) the loss function; and 4) the interrelationship between the predicted and observed concentrations (Belis et al., 2014; Crilley et al., 2017; Matthaios et al., 2021). The introduction of Na, Mg, Mn, Br, Sn and Ba as "weak species" in PMF which resulted in their uncertainties being increased by a factor of 3 produced more realistic profiles for the fine fraction (Amato and Hopke, 2012). PM mass was also included into the PMF to further aid the source characterisation. Additionally we included the unmeasured PM mass (UMPM) alongside the measured species in the input matrix (Hopke et al., 2003; Zhao et al., 2007). This UMPM was mainly to account for particle nitrate that could not be assessed in this study. The UMPM was defined as the observed sum of species (bulk fine or coarse PM concentration) mass minus the sum of all other measured species. The uncertainties were obtained as the square root of the sum of variances of all species involved in its determination and the variable was introduced as "weak" into the PMF with increased uncertainty by a factor of 3. Details of in-depth investigation of PMF optimal solution can be found in the supplementary material. Briefly, to evaluate the reproducibility of the PMF solutions and the adequacy of the number of PMF factors, a bootstrap, a displacement and a bootstrap-displacement technique were applied. Bootstrap is where random blocks of observations from the original dataset were sampled until reaching the size of the original input data. The bootstrap model method executed 100 iterations by using a random start and a minimum Pearson correlation coefficient of 0.6 (Belis et al., 2014; Bourtsoukidis et al., 2020). All the bootstrap modelled factors were well-reproduced for at least 95% of runs, indicating that the model uncertainties can be interpreted. Displacement technique explores the rotational ambiguity of the solution by assessing the largest range of source profile values, while the bootstrap-displacement is a combination of the former two and examines random errors in conjunction with rotational ambiguity. In both displacement validations no factor swaps were observed. In the bootstrap-displacement 94 and 91% of the coarse and fine PMF solutions were accepted, respectively and zero simulations experienced decreases in Q. For coarse simulations four and three factor swaps were observed while for fine simulations, four and two factor swaps were observed in the factors. Given the nature and complexity of these sources (often reported overlapping or not separated clearly in the literature; Amato et al., 2014b; Padoan and Amato, 2018; Harrison et al., 2021) and despite some small factor swaps, the overall PMF validation results for 6 and 7 solutions in coarse and fine PM is considered good. The number of factors is also considered appropriate as indicated by Figures S1 and S2 despite some species-specific elevated uncertainties in the respective solutions. The summary results of the evaluation techniques are listed in Table S1 and S2. To address the unexplained portion in PMF, a regression analysis between the obtained PMF factor values against the measured coarse and fine mass concentrations was applied. The R^2 between the PM concentrations predicted using the PMF model and those measured was 0.852 and 0.835 for coarse and fine PM, respectively, indicating good agreement (Figure S3).

2.3 Stepwise general additive model analysis

To investigate the parameters that affect roadside PM non-exhaust emission sources, a Stepwise General Additive Model (sGAM) regression technique was applied (Hastie, 2020). GAM can be substantially more flexible giving better overall predictions to linear and generalised linear models (Sofowote et al., 2021) because the relationships between independent and dependent variable are not assumed to be linear. GAM models are especially useful when the relationships between response variables and covariates are not known (Hastie and Tibshirani, 1990). sGAM is a step-by-step iterative construction of a regression model that involves the selection of independent variables based upon comparisons with all possible models that can be created based upon an identified set of predictors. A bidirectional elimination sGAM was used, which is a combination of forward selection and backward elimination models that test variables that should be included or excluded. In other words, a series of models is fitted, each corresponding to a formula obtained by moving each of the terms one step up or down in its regimen, relative to the formula of the current model. If the current value for any term is at either of the extreme ends of its regimen, only one rather than two steps are considered (Hastie, 1992). The best model is determined by the Akaike information criterion (AIC), which estimates the quality of each model relative to each of the other models. The entire process is repeated until either the maximum number of covariates has been used, or until the AIC criterion cannot be further decreased. In sGAM, we used distance from road, temperature, wind speed, relative humidity, number of vehicles and seasonality as numerical variables, while time (rush hours/non-rush hour), road type (A1, A2, A3), speed limit (40, 50, 60) and number of lanes (2, 4, 6, 8) were used as categorical variables. Each covariate in the sGAM could exist in three forms, either appear not at all, linearly, or as a smooth function estimated non-parametrically (Hastie, 2020). To identify the importance of individual predictors in the final GAM models we fitted alternative GAM models without each term (of the final sGAM model), and calculated the reduction in deviance which can also be translated as a measurement of the relative proportion of the variability in response variable explained by each covariate (Kuhn et al., 2015).

3. Results and discussion

In the coarse PM 21 elements were detected, while in fine PM 18 elements were identified. The mean concentrations and standard deviations for each element are shown in Table S3. The most abundant elements in coarse fraction were (in order) Si, Fe, Al, Cl and Ca, and in the fine fraction S, Cl, Si, Fe, Al which are primarily typical of crustal regional or marine origin, while anthropogenic elements such as Cu, Zn, K and Pb had lower concentrations.

3.1 Roadway ambient $PM_{10-2.5}$ and $PM_{2.5-0.2}$ source apportionment

Figure 2 shows the sources of $PM_{10-2.5}$ (coarse) and $PM_{2.5-0.2}$ (fine), respectively, for the greater Boston area near roadway pooled samples. Overall, the PMF analysis identified six $PM_{10-2.5}$ sources, namely: Salt aerosol, tyre-road abrasion, exhaust, regional pollution, road dust resuspension and brake wear, and seven $PM_{2.5-0.2}$ sources, namely: salt aerosol, brake wear, tyre-road abrasion, regional pollution, road dust resuspension, exhaust, and a factor rich in Cr and Ni. Combined non-exhaust emissions dominated the coarse fraction and accounted for 65.6% of their mass, while the exhaust particles accounted for 10.4% with 4% of their mass being unexplained by the PMF. In the fine PM fraction, exhaust particles accounted for 20.7% of the mass, while non-exhaust sources accounted for 29.1% with 2% of the mass to be unexplained by PMF. It should be noted that nitrate was not measured in this study however it is an important component in the near-road PM budget and in the US can contribute up to 17% and between 6% - 10% in the $PM_{10-2.5}$ and $PM_{2.5-0.2}$ fractions, respectively (Jeong et al., 2019; Habre et al., 2021). Here, the UMPM variable that included in the model was assumed to account mainly for the nitrate that was not measured in this study.

Salt aerosol: This is a distinct source characterised by high Cl and Na and relatively high Br (Belis et al., 2013). Major contribution to the enhancement of this factor (Figure S5) was from sea spray contributions in the summer months. The ratio of Na/Cl for coarse and fine PM was 0.47 and 0.68, respectively, indicating fresh sea salt (Crilley et al., 2016). However, a significant amount of Cl and Mg on Boston roads in the winter also comes from road de-icing salt (Matthaios et al., 2021). The Na/Mg ratio in coarse and fine fraction was 6.4 and 5.2, respectively which shows the high influence of fresh magnesium chloride salt typically used on roadways by the state of Massachusetts before and during snow storms in order to prevent snow and ice from sticking to the roads. Mg in the coarse fraction had a clear seasonal variation peaking during the winter months, however no seasonal variability was observed for the fine fraction. This source accounted for 7.9% and 5.0% of the coarse and fine PM, respectively.

Brake wear: In this source, in the coarse fraction, tracer metals typically used in brake pads were found in abundance. Zr, Cu and Ba, which are typical tracers for brake wear (Harrison et al., 2013), with percentages greater than 60%, while Ti, V, Cr and Fe were also elevated (>32%) compared to other factors. In the fine fraction, brake wear had similar tracers in abundance with Cu, Ba, Ti and Fe having 52.8%, 81.9%, 55.9% and 51.2% of their mass, respectively, assigned into this factor. Sr could not be detected in the fine fraction. For brake wear, the Cu/Sb ratio has also been used as a tracer (Pant and Harrison, 2013; Amato et al., 2016). However, in this study Sb was below the detection limit and could not be included in the analysis. Nevertheless, other brake wear characteristic ratios such as Cu/Fe, Cu/Sn and Cu/Mn were examined and had values of 0.056 (same for $PM_{2.5-0.2}$), 7.2 ($PM_{2.5-0.2}$: 4.6) and 5.0 ($PM_{2.5-0.2}$: 6.1) in the coarse and fine fractions respectively, which is in agreement with previous studies (Amato et al., 2011; Boogaard et al., 2011; Charron et al., 2019). Brake wear particles contributed 19.6% of the coarse and 7.7% of the fine roadway PM.

Road dust resuspension: In the coarse fraction, this source was identified by the high contribution of earth crustal elements, such as Al and Si, which were in abundance and greater than 54% in this factor. Mg, Fe and Mn were also in high percentages 32%, 33.7% and 44.5%, respectively. In the fine fraction, this source profile was rich in Si (48.4%) and Ca (62.7%). Both coarse and fine road dust sources had key tracer elements of other exhaust and non-exhaust sources in quantities ranging from 18 – 30%. This factor (and road dust in general) is influenced by settled particles from other vehicle sources such as brake lining wearing, catalyst degradation and exhaust, hence the elevated contributions of these elements in this profile. For example V, Cr, Ti and Zr, Sn, Ba which are often related to brake wear, were abundant in this source, while OC (18.7%) which is mainly an abrasion tracer and K (20.6%) which is a combustion related element were also notable in the coarse and (to a lesser degree) in the fine fraction. Similar enrichments in elements were found in other road dust studies (Adamiec, 2017; Zannoni et al., 2016). This source accounted for 29.6% and 9.1% of the PM_{10} and $PM_{2.5}$ roadway PM, respectively, and can be highly variable in both particle sizes depending not only upon road conditions and fleet composition but also on nearby activities and climatic conditions (Rienda and Alves, 2021).

Exhaust: This source was distinguished by the high loadings in carbon (EC and lesser OC) which is a typical tracer for combustion engines (Balasubramanian and Lee, 2007; Matthaios et al., 2021). The coarse fraction had a high EC loading, accounting for 67.6%. Coarse OC also had elevated values, 33.2%. Zn was also notable with 31% in the coarse and 19.6% in the fine and has been associated in the past with motor oil (*i.e.* Lough et al., 2005). Similar to the coarse PM, the fine fraction also had higher EC (73.2%) and OC (49.9%) percentages. Sn (23%) in the fine fraction was likely wrongly attributed to this factor (most likely due to source overlapping) since, as discussed above, it has a characteristic Cu/Sn ratio for brake wear. Exhaust source profile had three and four swaps with brake wear and regional pollution in coarse and fine fraction respectively. Exhaust $PM_{10-2.5}$ accounted for 10.4% of their mass and was the second most important source in the $PM_{2.5-0.2}$ accounting for 20.7% of their mass. The results for both coarse and fine PM are in agreement with most EU countries where non-exhaust emissions account for the greatest roadside PM percentage.

Regional pollution: This factor had very similar patterns in ambient coarse and fine fractions. This S-rich factor is predominantly composed of S, accounting for 52.3% and 81.5% of the coarse and fine S respectively and likely corresponds to secondary sulfate, consistent with the results of many previous source apportionment studies (Viana et al., 2007; Visser et al., 2015). The factor also comprises high relative contributions to K (49.4% and 40.5%) and Pb (50.2% and 35.6%) in the two fractions, respectively, and relatively high OC (30.1% and 21.7%) and EC (30.7% and 20.9%). High S loading in the fine fraction in Boston is mainly due to regional and long range transport of oil and coal combustion source emissions (Masri et al., 2015; Carrion-Matta et al., 2019), and is often used as a proxy for outdoor pollution infiltration indoors (Sarnat et al., 2002; Huang et al., 2018; Matthaios et al., 2021). The S/K ratios in biomass burning aerosols range from 0.5 (for fresh sources) to as high as 8 after transport and ageing of the emissions (Viana et al., 2013). The 2.93 and 7.4 S/K ratios obtained in this study for coarse and fine particles, respectively, suggest that fresh and aged biomass burning and coal combustion contribute differently to these fractions. This is supported by Figures S4 and S5, which show the factor contribution by distance from the road, indicating relatively fresher sources (such as biomass burning) contribute more in the coarse PM, while aged sources (such as long-range transport of coal combustion) contribute more to fine PM. The EC/OC ratio was also different for coarse (0.08) and fine (0.15) PM, supporting relatively fresh and aged source ratios, respectively (Reid et al., 2005). Pb has also been reported to be enriched in this factor possibly due to other local combustion sources and due to the bioaccumulation of Pb (Viana et al., 2008; Vassura et al., 2014). This factor accounted for 12.1% of the coarse mass and was the biggest factor in the fine fraction, accounting for 41.2%.

Tyre-Road abrasion: Coarse and fine tyre-road abrasion particles had different chemical profiles but both profiles were elevated in OC (12.9% coarse and 14.7% fine). The coarse fraction had high contribution of Ca (with 62% loading) which is an element that is used during road construction and can be used as a tracer for paved road wear (Piscitello et al., 2021), however no clear road construction contribution or soil tilling could be identified (Figure S4). The coarse fraction was also enriched in Sr (26.3%) and Mn (22.8%), which come from brake linings and asphalt pavement materials (Adachi and Tainosho, 2004; Kreider et al., 2010). Both coarse and fine fractions had high Zn (55.8% and 62.9%), respectively, which is used in tyre manufacturing in the form of ZnO and is widely considered a tracer for tyre wear in the near-road environment (Pant and Harrison, 2013; Harrison et al., 2012). The fine fraction also accounted for 40.9% of Al, while Mn (32.3%) and Sn (26.5%) were also notable. Despite often reported overlapping with other non-exhaust traffic-related sources, tyre-road abrasion source had no correlation with the road dust resuspension source or brake wear source in coarse and fine PMF profiles and accounted for 16.4% and 12.3% of their mass, respectively.

Cr and Ni factor: This factor was only found in the fine fraction with high relative contributions for Cr (81.6%) and Ni (86.4%), while notable was Mn (20.8%), Fe (20.8%) and Zn (13.7%). Similar source profiles were found in $PM_{2.5}$ in highways (Amato and Hopke, 2012), and urban environments (Vesser et al., 2015; Rai et al., 2020) while their profiles have been associated with traffic-related, industrial activities, waste incineration, solid waste dumping and oil combustion. Ni sources may include lubricating oil burning and heavy fuel oil used in industries and ships. Mn is used as an additive in vehicular fuel, while Cr and Ni may be derived from vehicle fuel combustion processes (Ntziachristos et al., 2007; Song and Gao, 2011). However, this factor had negative correlations with combustion (EC, OC, TC, K) and non-exhaust traffic-related (Cu, Ba, Zn, Zr, Ca, Si) elements and showed contributions when sampling at greater road distances (Figure S5), indicating its local or regional origin might be due to industrial activities. This factor was relatively small accounting only 2.0% of the fine mass.

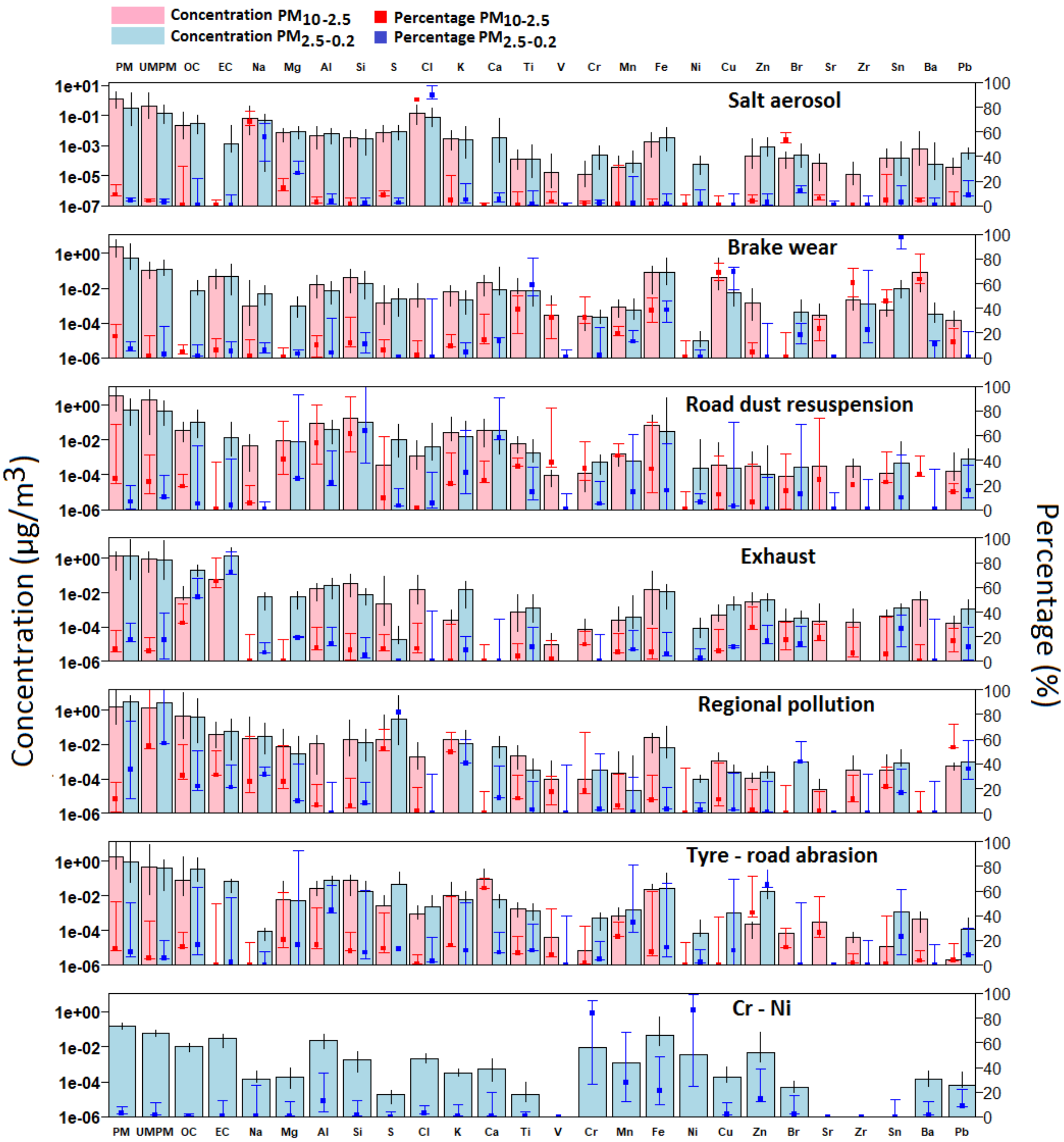

Figure 2: Source apportionment profiles (species percentages and concentrations in μg/m^3) for roadway $PM_{10\text{-}2.5}$ (red) and $PM_{2.5\text{-}0.2}$ (blue). The error bars show the 5th – 95th uncertainties from the bootstrap-displacement simulation.

3.2 Comparison with other near-road PM source apportionment studies

Table 3 shows the results from near-road PM sources around the globe. In this study we quantified the roadway PM with PMF source apportionment using measurements obtained using a mobile platform. Our results indicated that 65.6% of the coarse roadway PM is due to vehicle non-exhaust traffic-related emissions. Road dust resuspension was the biggest contributor, accounting for 29.6% of the coarse PM. Other studies that could separate the non-exhaust traffic-related emissions also found that road dust resuspension had higher contributions to near-road PM in France (Amato et al., 2014), Turkey (Karsi et al., 2020), China (Zhong et al., 2020), UK (Harrison et al., 2012) and Switzerland (Bukowiecki et al., 2010). For fine PM, road dust only accounted for 9.1% and was typically lower than other studies in the USA (Oakes et al., 2016; Habre et al., 2021), Europe (Amato et al., 2014b) and Asia (Zhang et al., 2020) where the fine road dust sources varied between 14 and 31%. However, this difference may be in part due to the fact that we sampled roadway PM at various distances from the main road (up to 750 m). Coarse brake wear emissions were slightly elevated compared to those reported for UK and Turkey tunnels (Lawrence et al., 2013; Karsi et al., 2020) and double compared to those reported for Russia (Vlasov et al., 2021); however, they were lower than those reported in urban roads and street canyons (Bukowiecki et al., 2010; Harrison et al., 2012; Amato et al., 2016; Song and Gao, 2011), likely due to the more aggressive and frequent use of brakes (Beji et al., 2020). In the fine fraction our results are on the same scale with those reported for four Chinese megacities by a Chemical Mass Balance (CMB) model (Zhong et al., 2020) but significantly lower than those reported for Canadian cities with Principal Component Analysis (PCA) (Dabek-Zlotorzynska et al., 2019). Our results also identified a tyre-road abrasion source which was analogous to findings of a PMF study in California (Habre et al., 2021); however, it was much smaller than those reported for Detroit and New Jersey with PCA analysis (Song and Gao, 2011; Oakes et al., 2016). For the same source in the fine fraction, our results were again lower than those reported for Detroit and were greater than the road in California (Table 1), which might be related to the different sampling distances from the road. Exhaust PM accounted for 10.4% of the coarse particles and was the second most important source in the fine fraction accounting for 20.7% of their mass. Larger numbers than this study were observed for the coarse fraction in both Europe and in China, while for fine fraction the numbers of this study were similar to those found in other US and European cities. It should be noted, however, that the direct comparisons of these studies have huge uncertainties, not only in terms of the analytical/statistical methods (PMF, CMB model and PCA), but also due to the fleet composition, road type and sampling conditions.

Table 1. Near-road PM source apportionment studies across the world. *: TSP; **: Road dust samples $^{+}$: includes both coarse and fine fraction.

Study	Location	Sampling location	Source apportionment technique	Year	% Contribution to PM mass				
					Exhaust	Brake wear	Tyre wear	Tyre-road wear	Road dust resuspension
Coarse PM									
This study	Boston, USA	Mobile platform	PMF	2018-19	10.4	19.6	-	16.4	29.6
Harrison et al., 2012	London, UK	Roadside site	Enrichment ratio	2007-11	-	55.3	10.7	-	38.1
	Granada, Spain				20	-	8	-	24
Amato et al., 2014b	Malaga, Spain	Roadside site	PMF	2003-10	19	-	-	-	21
	Sevilla, Spain				20	-	-	-	35
Lawrence et al., 2013	Hatfield,UK	Tunnel	PCA	2006	33	11	-	11	27
Karsi et al., 2020	Ankara, Turkey	Tunnel	PCA	2018	16.8*	13.9*	-	21.8*	33.4*
Oakes et al., 2016	Detroit, USA	Near road	PCA	2010	-	-	-	37	34
Habre et al., 2021	California, USA	Near road	PMF	2008-09	-	-	-	18	-
Song and Gao, 2011	New Jersey, USA	Near road	PCA	2007-08	28.3^{+}	35^{+}		23.7^{+}	
Amato et al., 2016	Paris, France	Road dust & near road	PMF	2012-13	47	30**	-	36**	13
Bukowiecki et al., 2010	Zurich, Switzerland	Urban street canyon	PMF	2007	41	21	-	-	38
		Freeway			41	3	-	-	56
	Beijing, China				25	1	5	-	69
Zhang et al., 2020	Tianjin, China	Tunnel	CMB	2017-18	28	3	4	-	65
	Qingdao, China				39	1	9	-	54
Vlasov et al., 2021	Moscow, Russia	Road dust	PCA	2017	-	7.2	6.3	7.0	-
Fine PM									
This study	Boston, USA	Mobile platform	PMF	2018-19	20.7	7.7	-	12.3	9.1
	Granada, Spain				18	-	18	-	22
Amato et al., 2014b	Malaga, Spain	Roadside	PMF	2003-10	12	-	-	-	21
	Sevilla, Spain				19	-	-	-	31
Dabek-Zlotorzynska et al., 2019	Vancouver &Toronto. Canada	Near road	PCA	2015-16	12	55	-	-	11
Oakes et al., 2016	Detroit, USA	Near road	PCA	2010	-	-	-	31	18
Habre et al., 2021	California, USA	Near road	PMF	2008-09	20.9	-	-	11.4	-
	Beijing, China			2017-18	80	1	6	-	14
Zhang et al., 2020	Tianjin, China	Tunnel	CMB		59	3	4	-	34
	Zhengzhou, China				80	5	3	-	11
	Qingdao, China				68	2	6	-	22

3.3 Factors affecting exhaust and non-exhaust roadway PM

The results for the factors that affect the coarse and fine roadside exhaust and non-exhaust traffic-related PM with the implementation of sGAM technique are shown in Tables 2 and 3. The analysis showed that exhaust and non-exhaust traffic-related sources are affected by different factors in coarse and fine PM when using models that include both linear and non-linear covariates. Overall sGAMs predicted better the coarse exhaust and non-exhaust traffic-related sources explaining 47.5 – 81.6% of their variability, while fine sGAM models for the same sources explained 13.6 – 83.7%.

Road dust resuspension source had wind speed, temperature, relative humidity and time as common covariates in the coarse and fine sGAMs. Wind speed was the most important predictor in this source having both linear and smoothing implementations. Wind speed was significantly ($p < 0.05$) associated with this source for both coarse and fine PM, with a relative importance (importance of the predictor out of the total variance explained) of 47.2% and 40.8%, respectively. Temperature was also a notable predictor explaining 30.3% and 21.3% of sGAMs variability with significantly ($p < 0.05$) and partially significantly ($p < 0.1$) associations in the coarse and fine fractions, respectively. Relative humidity was also significantly associated with this source, accounting for similar variability in the coarse (8%) and fine (7.2%) sGAMs. These results are in agreement with Padoan and Amato (2018) and Rienda and Alves (2021), where dry conditions were found to enhance the resuspension of road dust. In both fractions, this source was significantly ($p < 0.05$) negatively associated with time of day (greater in rush hours) and had relative importance in sGAM of 4.4% and 30.7% for coarse and fine fractions, respectively. Speed limit was only significantly associated with the coarse road dust resuspension source having 10.1% relative importance. Traffic related resuspension is influenced by vehicle wake turbulence (Harrison et al., 2021), which in turn can be exacerbated by vehicle speed.

Road-tyre abrasion for both coarse and fine fractions was significantly positively associated with temperature, time and number of vehicles. Temperature was equally important for the coarse and fine PM with similar relative importance of 21.5% and 19.1%, respectively. Higher temperatures often relate to drier conditions, which in conjunction with more vehicles promote more road wear and make the tyres wear faster due to the greater temperature during contact of the tyre with the road surface (Park et al., 2017). In $PM_{10-2.5,}$ this source was further significantly associated with speed limit and inverse associated with distance from the road. Greater speeds, abrupt cornering and braking have been associated with greater tyre particles (Kwak et al., 2014) which are common driving characteristics in congested urban roads (Beji et al., 2021).

The exhaust source in both fractions was significantly associated with temperature and time of day. Temperature had a relative importance of 35.7% and 71.5% and had a smooth implementation and an inverse linear association with coarse and fine PM, respectively. At lower ambient temperatures, the engine and catalyst warm-up period is prolonged often leading to inefficient combustion, inefficient catalyst operation, and the potential for the vehicle to be operating under fuel-rich conditions, which has an adverse effect on vehicle exhaust emissions (Nam et al., 2010; Matthaios et al., 2019). Time of day was associated with both exhaust $PM_{10-2.5}$ and $PM_{2.5-0.2}$ and had a relative importance of 37.1 and 17%, respectively. Rush hour periods were found to have greater overall emissions (Requia et al., 2018). Different road types and greater numbers of road lanes together had a relative importance of 27% for exhaust $PM_{10-2.5}$, while number of vehicles had a significant positive association and a relative importance of 12.5% for fine PM.

Brake wear $PM_{10-2.5}$ and $PM_{2.5-0.2}$ are significantly positively associated with temperature and number of vehicles on the road which combined had a relative importance of 57.8% and 46.9%, respectively. $PM_{10-2.5}$ was further inversely associated with time of day, which was the most important predictor with 42.2% relative importance. The positive association with number of vehicles (in both fractions) and negative association with time of day (in the coarse fraction) and distance from the road (in fine fraction) shows that urban roads during congested periods such as morning rush hours can promote the frequent use of brakes, therefore create more brake wear on the road. Brake pads and discs are composed of a wide range of materials which are influenced by several parameters (Grigoratos and

Martini, 2015). Temperature is recognized as an important factor for brake wear emissions and greater ambient temperature (significantly associated with coarse and fine PM; Tables 2 and 3) might enhance the chance of a braking pad to pass the critical temperature (120-200°C; Kukutschová et al., 2011; Nosko et al., 2017; Perricone et al., 2018) and generate more wear debris through abrasion of the pad with the disc (Verma et al., 2016; Alemani et al., 2017).

Overall, the explained variability by sGAMs was better for the coarser than fine exhaust and non-exhaust traffic-related sources. sGAMs predicted well the tyre-road abrasion source in both coarse and fine fractions having common predictors of temperature, number of vehicles and time of day that explained 81.6% and 83.7% of its variability, respectively. Other sGAM results for coarse and fine vehicle sources varied significantly. Notable was the difference in road dust resuspension where, despite having wind speed, temperature, relative humidity and time of day as common predictors, the variability explained by sGAMs was 77% and 13.6% for coarse and fine particles, respectively and did not improve even after adding only smooth approximation covariates in the fine fraction. It should be mentioned that part of the unexplained variability by our approach might be due to the limitations of the study which included only 90 sample measurements, which were unable to account for both within day and between day variability. Furthermore, further research is needed to isolate factors that affect these sources under real-world driving conditions, as the results of the models in this study only represent snapshots of the actual factors that may influence these sources. Variables such as road inclination (uphill/downhill), vehicle fleet composition (heavy duty/passenger/light duty vehicles), driving speed, green space or building height, which were not included, could explain some of the variability of these sources and improve the predictive power of sGAMs.

Table 2. Multiple linear regression for each $PM_{10-2.5}$ profile sources; VIF: Variance inflation factor for linear predictors: values close to 10 indicate co-linearity; % relative importance (R.I.): importance of the predictor out of the total variance explained; + indicates non-parametric GAM variables; underlined values indicate significance at p <0.1; * and ** indicate significance levels p <0.05 and p <0.01 respectively.

Variable	Coefficient (± std error)	VIF	R.I. of predictor (%)
Exhaust $PM_{10-2.5}$			
Road type	3.8e-01±0.1.8e-01*	4.45	7.0
Number of lanes	2.1e-01±7e-02**	4.94	20.2
Temperature+	1.73**	-	35.7
Time+	1.71**	-	37.1
Adjusted R^2 (% deviance explained)	0.436 (47.5)		
Dust resuspension $PM_{10-2.5}$			
Wind speed+	2.73**	-	47.2
Speed limit	4.1e-02±1.0e-02**	2.22	10.1
Relative humidity+	1.65*	-	8.0
Temperature+	1.89**	-	30.3
Time	<u>-2.5e-01±6.3e-01</u>	1.13	4.4
Adjusted R^2 (% deviance explained)	0.745 (77.0)		
Road-tyre abrasion $PM_{10-2.5}$			
Number of vehicles	1.2e-04±2.2e-05**	2.08	42.1
Speed limit+	3.87***	-	20.6
Distance from the road	-1.5e-02±2.4e-03**	4.89	10.0
Temperature	6.6e-02±2.0e-02**	1.25	21.5
Time	-6.6e-01±1.8e-01**	1.84	5.8
Adjusted R^2 (% deviance explained)	0.842 (81.6)		
Brake wear $PM_{10-2.5}$			
Number of vehicles	5.8e-04±2.3e-04*	2.45	34.6
Temperature	1.8e-01±2.3e-02**	1.23	23.2
Time	-3.1e-01±5.6e-02**	1.01	42.2
Adjusted R^2 (% deviance explained)	0.814 (76.2)		

Table 3. Multiple linear regression for each $PM_{2.5-0.2}$ profile source; VIF: Variance inflation factor for linear predictors: values close to 10 indicate co-linearity; % relative importance (R.I.): importance of the predictor out of the total variance explained; + indicates non-parametric GAM variables; underlined values indicate significance at p <0.1; * and ** indicate significance levels p <0.05 and p <0.01 respectively.

Variable	Coefficient (±std error)	VIF	R.I of predictor (%)
Exhaust $PM_{2.5-0.2}$			
Temperature	-2.3e-02±6.3e-03**	1.03	71.5
Time	-1.8e-01±1.08e-01	1.01	16.0
Number of vehicles	6.0e-04±1.5e-04	1.19	12.5
Adjusted R^2 (% deviance explained)	0.205 (23.4)		
Dust resuspension $PM_{2.5-0.2}$			
Time	-9.1e-01±3.3e-01*	1.05	30.7
Temperature	4.4e-03±3.2e-03	1.84	21.3
Wind speed	1.8e-01±7.9e-02**	2.15	40.8
Relative humidity	-3.1e-02±1.4e-02*	3.20	7.2
Adjusted R^2 (% deviance explained)	0.113 (13.6)		
Road-tyre abrasion $PM_{2.5-0.2}$			
Temperature$^+$	1.84**	-	19.1
Time	-7.2e-02±2.2e-03	2.55	40.1
Number of vehicles	2.1e-04±1.1e-04	1.12	40.8
Adjusted R^2 (% deviance explained)	0.855 (83.7)		
Brake wear $PM_{2.5-0.2}$			
Temperature$^+$	1.471	-	26.8
Number of vehicles	1.37e-04±2.4e-05**	1.24	20.1
Relative humidity	-3.6e-02±1.6e-02**	1.52	13.7
Distance from the road$^+$	1.803**	-	39.4
Adjusted R^2 (% deviance explained)	0.232 (27.4%)		

4. Conclusions

The study deployed a mobile platform and investigated the sources of ambient air roadway coarse and fine PM in the greater Boston area. PMF was applied to roadway samples and identified six coarse and seven fine sources. Sources for both coarse and fine PM included road salt, exhaust, regional pollution, brake wear, road dust resuspension and tyre-road abrasion. An additional source for fine PM was a source rich in Cr and Ni. Non-exhaust traffic-related sources accounted for 65.6% and 29.1% of the coarse and fine PM, respectively, while exhaust PM was the second most important source in the fine fraction, accounting for 20.7%. The application of stepwise general additive models to investigate factors that affect these sources showed that temperature was significant in all vehicle-related sources and had a relative importance between 3.2 - 35.7% and 19.1 - 71.5% for $PM_{10-2.5}$ and $PM_{2.5-0.2}$, respectively. The other two important predictors, significant in three out of four vehicle-related sources, were rush hour periods and number of vehicles. Meteorological variables of relative humidity and wind speed were important predictors only for coarse and fine road dust resuspension, while speed limit was an important predictor only for coarse road dust resuspension and tyre-road abrasion sources. Overall, the models could predict better the coarse vehicle-related sources with R^2 varying from 0.44 to 0.84, while fine R^2 varied between 0.11 and 0.86. These results show the complexity and the challenges of identifying potential predictors or mitigating factors that may affect and potentially reduce the emissions of non-exhaust traffic-related emission sources. However, with the increasing share of electric vehicles in the fleet, these emissions are becoming a more significant contributor to the near-road PM composition, where the quantitative approaches of this study may help improve vehicle emission inventories.

Acknowledgements

Research described in this article was conducted under contract to the Health Effects Institute (HEI), an organization jointly funded by the United States Environmental Protection Agency (U.S. EPA) (Assistance Award No. CR-83467701) and certain motor vehicle and engine manufacturers. The contents of this article do not necessarily reflect the views of HEI, or its sponsors, nor do they necessarily reflect the views and policies of the EPA or motor vehicle and engine manufacturers. This publication was made possible by U.S. EPA grant RD-83587201. Its contents are solely the responsibility of the grantee and do not necessarily represent the official views of the U.S. EPA. Further, U.S. EPA does not endorse the purchase of any commercial products or services mentioned in the publication.

References

Acosta, J. A., Faz, A., Kalbitz, K., Jansen, B., Martínez-Martínez, S., 2011. Heavy metal concentrations in particle size fractions from street dust of Murcia (Spain) as the basis for risk assessment. J. Environ. Monit. 13, 3087–3096. https://doi.org/ 10.1039/c1em10364d.

Adachi K., Y. Tainosho Y., Characterization of heavy metal particles embedded in tire dust Environ. Int., 30 (2004), pp. 1009-1017, 10.1016/j.envint.2004.04.004.

Adamiec, E., 2017. Chemical fractionation and mobility of traffic-related elements in road environments. Environ. Geochem. Health 39, 1457–1468. https://doi.org/ 10.1007/s10653-017-9983-9.

Alemani, M.; Gialanella, S.; Straffelini, G.; Ciudin, R.; Olofsson, U.; Perricone, G.; Metinoz, I. Dry sliding of a low steel friction material against cast iron at different loads: Characterization of the friction layer and wear debris. Wear 2017, 376–377, 1450–1459.

Amato, F., Hopke, P.K., 2012. Source apportionment of the ambient PM2.5 across St. Louis using constrained positive matrix factorization. Atmos. Environ. 46, 329–337. https://doi.org/10.1016/j.atmosenv.2011.09.062.

Amato, F., M. Viana, A. Richard, M. Furger, A. S. H. Prévôt, S. Nava, F. Lucarelli, N. Bukowiecki, A. Alastuey, C. Reche et al. 2011. Size and time-resolved roadside enrichment of atmospheric particulate pollutants. Atmos. Chem. Phys. 11 (6):2917. doi:10.5194/acp-11-2917-2011.Amato, F., Cassee, F. R., Denier van der Gon, H. A. C., Gehrig, R., Gustafsson, M., Hafner, W., et al. (2014a). Urban air quality: The challenge of traffic non-exhaust emissions. Journal of Hazardous Materials, 275, 31-36. http://dx.doi.org/10.1016/j.jhazmat.2014.04.053.

Amato, F., Alastuey, A., de la Rosa, J., Gonzalez Castanedo, Y., Sánchez de la Campa, A. M., Pandolfi, M., Lozano, A., Contreras González, J., and Querol, X. (2014b): Trends of road dust emissions contributions on ambient air particulate levels at rural, urban and industrial sites in southern Spain, Atmos. Chem. Phys., 14, 3533–3544, https://doi.org/10.5194/acp-14-3533-2014, 2014.

Amato, F., Favez, O., Pandolfi, M., Alastuey, A., Querola, X., Moukhtarc, S., et al. (2016). Traffic induced particle resuspension in Paris: Emission factors and source contributions. Atmospheric Environment, 129, 114-124.http://dx.doi.org/10.1016/j.atmosenv.2016.01.022.

Balasubramanian, R., & Lee, S. S. (2007). Characteristics of Indoor Aerosols in Residential Homes in Urban Locations: A Case Study in Singapore. Journal of the Air & Waste Management Association, 57(8), 981–990.

Beji, A., Deboudt, K., Khardi, S., Muresan, B. et al., Determinants of Rear-of-Wheel and Tire-Road Wear Particle Emissions by Light-Duty Vehicles using On-Road and Test Track Experiments," Atmospheric Pollution Research, 2020

Belis, C. a, Larsen, B. R., Amato, F., Haddad, I. El, Favez, O., Harrison, R. M., Hopke, P. K., Nava, S., Paatero, P., Prévôt, A., Quass, U., Vecchi, R. and Viana, M.: European Guide on Air Pollution Source Apportionment with Receptor Models., 2014.

Boogaard, H., Kos, G. P. A., Weijers, E. P., Janssen, N. A. H., Fischer, P. H., van der Zee, S. C., de Hartog, J. J., and Hoek, G.: Contrast in air pollution components between major streets and background locations: Particulate matter mass, black carbon, elemental composition, nitrogen oxide and ultrafine particle number, Atmos. Environ. 45, 650–658, 2011.

Bourtsoukidis, E., Pozzer, A., Sattler, T., Matthaios, V. N., Ernle, L., Edtbauer, A., Fischer, H., Könemann, T., Osipov, S., Paris, J.-D., Pfannerstill, E. Y., Stönner, C., Tadic, I., Walter, D., Wang, N., Lelieveld, J. and Williams, J.: The Red Sea Deep Water is a potent source of atmospheric ethane and propane, Nat. Commun., 11(1), 447, doi:10.1038/s41467-020-14375-0, 2020.

Bukowiecki, N., Lienemann, P., Hill, M., Furger, M., Richard, A., Amato, F., Prevot, A.S. H., Baltensperger, U., Buchmann, B., Gehrig, R., 2010. PM10 emission factors for non-exhaust particles generated by road traffic in an urban street canyon and along a freeway in Switzerland. Atmos. Environ. 44, 2330–2340. https://doi.org/10.1016/j. atmosenv.2010.03.039.

Carlsten, C., Dybuncio, A., Becker, A., Chan-Yeung, M., Brauer, M., 2011. Trafficrelated air pollution and incident asthma in a high-risk birth cohort. Occup. Environ. Med. 68 (4), 291e295.

Charron, A., Polo-Rehn, L., Besombes, J.L., Golly, B., Buisson, C., Chanut, H., Marchand, N., Guillaud, G., Jaffrezo, J.L., 2019. Identification and quantification of particulate tracers of exhaust and non-exhaust vehicle emissions. Atmos. Chem. Phys. 19, 5187–5207.

Crilley, L. R., Lucarelli, F., Bloss, W. J., Harrison, R. M., Beddows, D. C., Calzolai, G., et al. (2017). Source apportionment of fine and coarse particles at a roadside and urban background site in London during the 2012 summer ClearfLo campaign. Environmental Pollution, 220, 766-778. http://dx.doi.org/10.1016/j.envpol.2016.06.002.

Dabek-Zlotorzynska E., V. Celo, L. Ding, D. Herod, C.H. Jeong, G. Evans, N. Hilker, Characteristics and sources of PM2.5 and reactive gases near roadways in two metropolitan areas in Canada, Atmos. Environ. 218 (2019), 116980.

Gan, W.Q., Koehoorn, M., Davies, H.W., Demers, P.A., Tamburic, L., Brauer, M., 2011. Long-Term exposure to traffic-related air pollution and the risk of coronary heart disease hospitalization and mortality. Environ. Health Perspect. 119 (4), 501-507.

Gauderman, W.J., Vora, H., McConnell, R., Berhane, K., Gilliland, F., Thomas, D., Lurmann, F., Avol, E., Kunzli, N., Jerrett, M., Peters, J., 2007. Effect of exposure to traffic on lung development from 10 to 18 years of age: a cohort study. Lancet 369 (9561), 571-577.

Grigoratos, T., Martini, G., 2015. Brake wear particle emissions: a review. Environ. Sci. Pollut. Res. 22, 2491–2504.

Habre R., Girguis M., Urman R., Fruin S., Lurmann F., Shafer M., Gorski P., Franklin M., McConnell R., Avol E., Gilliland F., 2021. Contribution of tailpipe and non-tailpipe traffic sources to quasi-ultrafine, fine and coarse particulate matter in southern California, Journal of the Air & Waste Management Association, 71:2, 209-230, DOI: 10.1080/10962247.2020.1826366.

Harrison, R.M., Jones, A.M., Gietl, J., Yin, J., Green, D.C., 2012. Estimation of the contributions of brake wear, tire wear, and resuspension to nonexhaust traffic particles derived from atmospheric measurements. Environ. Sci. Technol. 46, 6523–6529.

Harrison, R.M., Beddows, D.C., 2017. Efficacy of recent emissions controls on road vehicles in Europe and implications for public health. Sci. Rep. 7, 1152. https://doi. org/10.1038/s41598-017-01135-2

Harrison et al., 2021 Non-exhaust vehicle emissions of particulate matter and VOC from road traffic: A review Atmospheric Environment 262, 118592 https://doi.org/10.1016/j.atmosenv.2021.118592

Hastie, T. J. (1992) Generalized additive models. Chapter 7 of Statistical Models in S eds J. M. Chambers and T. J. Hastie, Wadsworth & Brooks/Cole.

Hastie, T. and Tibshirani, R. (1990) Generalized Additive Models. London: Chapman and Hall.

Hastie T., (2020) R package 'gam'Generalised Additive Models Version 1.09 (http://cran.r-project.org/web/packages/gam/ index.html)

Hopke, P.K., Ramadan, Z., Paatero, P., Norris, G.A., Landis, M.S., Williams, R.W., Lewis, C.W., 2003. Receptor modeling of ambient and personal exposure samples: 1998 Baltimore Particulate Matter Epidemiology-Exposure Study. Atmos. Environ. 37, 3289-3302. https://doi.org/https://doi.org/10.1016/S1352-2310(03)00331-5

Huang, S., J. Lawrence, C.-M. Kang, J. Li, M. Martins, P. Vokonas, D. R. Gold, J. Schwartz, B. A. Coull, and P. Koutrakis. 2018. Road proximity influences indoor exposures to ambient fine particle mass and components. Environ. Pollut. 243 (December): 978–87. doi:10.1016/j.envpol.2018.09.046.

Huang, S., Taddei, P., Lawrence, J., Martins, M. A., Li, J., & Koutrakis, P. 2020. Trace element mass fractions in road dust as a function of distance from road. Journal of the Air & Waste Management Association. doi:10.1080/10962247.2020. 1834011.

Jeong, C.H., Wang, J.M., Hilker, N., Debosz, J., Sofowote, U., Su, Y., Noble, M., Healy, R.M.,Munoz, T., Dabek-Zlotorzynska, E., Celo, V., 2019.Temporal and spatial variability oftraffic-related PM2.5sources: comparison of exhaust and non-exhaust emissions. Atmos. Environ. 198, 55–69

Karsi M.B.B., Berberler E., Berberler T., Aslan O., Yenisoy-Karakas S., Karakas D., 2020. Correction and source apportionment of vehicle emission factors obtained from Bolu Mountain Highway Tunnel, Turkey. Atmospheric Pollution Research Volume 11, Issue 12, December 2020, P 2133-2141.

Kreider M. L., Panko J. M., McAtee B. L., Sweet L. I., Finley B. L., Physical and chemical characterization of tire-related particles: comparison of particles generated using different methodologies Sci. Total Environ., 408 (2010), pp. 652-659, 10.1016/j.scitotenv.2009.10.016.

Kuhn M, Wing J, Weston S, et al. (2015) Package ―caret‖. Available from: http://caret.r-forge.r-project.org.

Kukutschová, J.; Moravec, P.; Tomášek, V.; Matějka, V.; Smolík, J.; Schwarz, J.; Seidlerová, J.; Šafářová, K.; Filip, P. On airborne nano/micro-sized wear particles released from low-metallic automotive brakes. Environ. Pollut. 2011.

Kwak, J., Lee, S., Lee, S., 2014. On-road and laboratory investigations on non-exhaust ultrafine particles from the interaction between the tire and road pavement under braking conditions. Atmos. Environ. 97, 195–205.

Lawrence, S., Sokhi, R., Ravindra, K., Mao, H., Prain, H. D., & Bull, I. D. (2013). Source apportionment of traffic emissions of particulate matter using tunnel measurements. Atmospheric Environment, 77, 548-557. http://dx.doi.org/10.1016/j.atmosenv.2013.03.040.

Lawrence, J., J. M. Wolfson, S. Ferguson, P. Koutrakis, and J. Godleski. 2004. Performance stability of the Harvard ambient particle concentrator. Aerosol Sci. Technol. 38 (3):219–27. doi:10.1080/02786820490261735.

Lough GC, Schauer JJ, Park J-S, Shafer MM, Deminter JT, Weinstein JP (2005) Emissions of metals associated with motor vehicle roadways. Environmental Science & Technology 39: 826-836

Martins, M., Lawrence, J., Ferguson, S., Wolfson, J. M., & Koutrakis, P. 2021. Development, and evaluation of a mobile laboratory for collecting short-duration near-road fine and coarse ambient particle and road dust samples. Journal of the Air & Waste Management Association. doi:10.1080/10962247.2020.1853626.

Masri S., Kang CM., Koutrakis P., (2015) Composition and sources of fine and coarse particles collected during 2002–2010 in Boston, MA, Journal of the Air & Waste Management Association, 65:3, 287-297, DOI: 10.1080/10962247.2014.982307

Matthaios, V.N., Kramer, L.J., Sommariva, R., Pope, F.D., Bloss, W.J., 2019. Investigation of vehicle cold start primary NO2 emissions inferred from ambient monitoring data in the UK and their implications for urban air quality. Atmos. Environ. 199, 402–414. https://doi.org/10.1016/j.atmosenv.2018.11.031

Matthaios, V. N., Liu M., Li L., Kang C. M., Viera C. L. Z., Gold D. R., Koutrakis P., 2021. Sources of indoor PM2.5 gross α and β activities measured in 340 homes. Env. Res. 197, 111114.

Nam, E.; Kishan, S.; Baldauf, R. W.; Fulper, C. R.; Sabisch, M.; Warila, J. Temperature Effects on Particulate Matter Emissions from Light-Duty, Gasoline-Powered Motor Vehicles. Environ. Sci. Technol. 2010, 44 (12), 4672−4677.

Norris G, Duvall R, Brown S, Bai S. EPA Positive Matrix Factorization (PMF) 5.0 Fundamentals and User Guide. US Environmental Protection Agency, Washington, DC, 2014.

Nosko, O.; Vanhanen, J.; Olofsson, U. Emission of 1.3–10 nm airborne particles from brake materials. Aerosol Sci. Technol. 2017, 51, 91–96.

Ntziachristos, L., Ning, Z., Geller, M.D., Sheesley, R.J., Schauer, J.J., Sioutas, C., 2007. Fine, ul-trafine and nanoparticle trace element compositions near a major freeway with ahigh heavy-duty diesel fraction. Atmos. Environ. 41, 5684–5696.https://doi.org/10.1016/j.atmosenv.2007.02.043.

Oakes, M. M., J. M. Burke, G. A. Norris, K. D. Kovalcik, J. P. Pancras, and M. S. Landis. 2016, November. Near road enhancement and solubility of fine and coarse particulate matter trace elements near a major interstate in Detroit, Michigan. Article. Atmos. Environ. 145:213–24. doi:10.1016/j.atmosenv.2016.09.034.

Pant, P., Harrison, R.M., 2013. Estimation of the contribution of road traffic emissions to particulate matter concentrations from field measurements: a review. Atmos. Environ. 77, 78–97.

Park I., Lee J., and Lee S., (2017) Laboratory study of the generation of nanoparticles from tire tread, Aerosol Science and Technology, 51:2, 188-197, DOI:10.1080/02786826.2016.1248757

Piscitello A., Bianco C., Casasso A., Sethi R., Non-exhaust traffic emissions: sources, characterization, and mitigation measures Sci. Total Environ., 766 (2021), Article 144440

Padoan, E., Amato, F., 2018.Vehicle non-exhaust emissions: impact on air quality. F.Amato, (Eds.) Non-Exhaust Emissions. An Urban Air Quality Problem for PublicHealth. Impact and Mitigation Measures. Elsevier.

Perricone, G.; Matějka, V.; Alemani, M.; Valota, G.; Bonfanti, A.; Ciotti, A.; Olofsson, U.; Söderberg, A.; Wahlström, J.; Nosko, O.; et al. A concept for reducing PM10 emissions for car brakes by 50%. Wear 2018, 396–397, 135–145.

Polissar, A. V., Hopke, P. K., Paatero, P., Malm, W. C., and Sisler, J. F.: Atmospheric aerosol over Alaska, 2. Elemental Composition and Sources, J. Geophys. Res.-Atmos., 103, 19045–19057, doi:10.1029/98JD01212, 1998.

Rai, P., Furger, M., El Haddad, I., Kumar, V., Wang, L., Singh, A., Dixit, K., Bhattu, D., Petit, J.E., Ganguly, D., Rastogi, N., Baltensperger, U., Tripathi, S.N., Slowik, J.G., Pr evˆot, A.S.H., 2020. Real-time measurement and source apportionment of elements in Delhi’s atmosphere. Sci. Total Environ. 742, 140332. https://doi.org/10.1016/j. scitotenv.2020.140332.

Reid, J.S., Koppmann, R., Eck, T.F., Eleuterio, D.P., 2005. A review of biomass burning emissions part II: intensive physical properties of biomass burning particles. Atmospheric Chemistry and Physics 5, 799-825

Requia W. J., Higgins C. D., Adams M. D., Mohamed M., Koutrakis P., 2018. The health impacts of weekday traffic: a health risk assessment of PM2.5 emissions during congested periods Environ. Int., 111 (2018), pp. 164-176.

Rienda I. C., Alves A. C., 2021 Road dust resuspension: A review. Atmospheric Research Volume 261, 105740 https://doi.org/10.1016/j.atmosres.2021.105740

Sarnat, J.A., C.M. Long, P. Koutrakis, B.A. Coull, J. Schwartz, H.H. Suh Using sulfur as a tracer of outdoor fine particulate matter Environ. Sci. Technol., 36 (2002), pp. 5305-5314

Silva E., Huang S., Lawrence J., Martins M. A. G., Li J., Koutrakis P., (2021) Trace element concentrations in ambient air as a function of distance from road, Journal of the Air & Waste Management Association, 71:2, 129-136, DOI: 10.1080/10962247.2020.1866711

Sioutas, C., P. Koutrakis, J. J. Godleski, S. T. Ferguson, C. S. Kim, and R. M. Burton. 1997. Fine particle concentrators for inhalation exposures—Effect of particle size and composition. J. Aerosol Sci. 28 (6):1057–71. doi:10.1016/S0021-8502(96)00493-4.

Sofowote, U.M., Healy, R.M., Su, Y., Debosz, J., Noble, M., Munoz, A., Jeong, C.-H., Wang, J.M., Hilker, N., Evans, G.J., Brook, J.R., Lu, G., Hopke, P.K., 2021. Sources, variability and parameterizations of intra-city factors obtained from dispersion-normalized multi-time resolution factor analyses of PM2.5 in an urban environment. Sci. Total Environ. 761, 143225. https://doi.org/10.1016/j.scitotenv.2020.143225

Song, F., Gao, Y., 2011. Size distributions of trace elements associated with ambientparticular matter in the affinity of a major highway in the New Jersey–NewYork metropolitan area. Atmos. Environ. 45, 6714–6723.https://doi.org/10.1016/j.atmosenv.2011.08.031.

USEPA, (2020). Brake and tire wear emissions from onroad vehicles in MOVES3, report of the United States environmental Protection agency, EPA-420-R-20-014, November 2020. https://nepis.epa.gov/Exe/ZyPDF.cgi/P1010M43.PDF?Dockey=P1010M43. PDF.

Vassura, I., Venturini, E., Marchetti, S., Piazzalunga, A., Bernardi, E., Fermo, P., Passarini, F.,2014. Markers and influence of open biomass burning on atmospheric particulatesize and composition during a major bonfire event. Atmos. Environ. 82, 218–225.

Verma, P.C.; Ciudin, R.; Bonfanti, A.; Aswath, P.; Straffelini, G.; Gialanella, S. Role of the friction layer in the high-temperature pin-on-disc study of a brake material. Wear 2016, 346–347, 56–65.

Viana, M., Querol, X., Götschi, T., Alastuey, A., Sunyer, J., Forsberg, B., Heinrich, J., Norbäck, D., Payo, F., Maldonado, J. A., and Künzli, N.: Source apportionment of ambient PM2.5 at five spanish centres of the European community respiratory health survey (ECRHS II), Atmos. Environ., 41, 1395–1406, 2007

Viana M., C. Reche, F. Amato, A. Alastuey, X. Querol, T. Moreno, F. Lucarelli, S. Nava, G. Calzolai, M. Chiari, M. Rico (2013). Evidence of biomass burning aerosols in the Barcelona urban environment during winter time. Atmospheric Environment. 72 81- 88.

Viana M., J.M. López, X. Querol, A. Alastueya, D. Garcıa-Gaciob, G. Blanco-Herasb, P. López,Mahía, M. Pineiro-Iglesias, M.J. Sanz, F. Sanz, X. Chi, W. Maenhau (2008). Tracers and impact of open burning of rice straw residues on PM in Eastern Spain. Atmospheric Environment. 42 1941 – 1957

Visser, S., Slowik, J. G., Furger, M., Zotter, P., Bukowiecki, N., Canonaco, F., Flechsig, U., Appel, K., Green, D. C., Tremper, A. H., Young, D. E., Williams, P. I., Allan, J. D., Coe, H., Williams, L. R., Mohr, C., Xu, L., Ng, N. L., Nemitz, E., Barlow, J. F., Halios, C. H., Fleming, Z. L., Baltensperger, U., Prévôt, A. S. H., 2015. Advanced source apportionment of sizeresolved trace elements at multiple sites in London during winter. Atmospheric Chemistry and Physics 15, 11291-11309.

Vlasov, D., Kosheleva, N., Kasimov, N., 2020. Spatial distribution and sources of potentially toxic elements in road dust and its PM10 fraction of Moscow megacity. Sci. Total Environ. 5, 143267. https://doi.org/10.1016/j.scitotenv.2020.143267.

Wilhelm, M., Ghosh, J.K., Su, J., Cockburn, M., Jerrett, M., Ritz, B., 2012. Traffic-related air toxics and term low birth weight in Los Angeles County, California. Environ. Health Perspect. 120 (1), 132-138.

Zannoni, D., Valotto, G., Visin, F., Rampazzo, G., 2016. Sources and distribution of tracer elements in road dust: The Venice mainland case of study. J. Geochem. Explor. 166, 64–72. https://doi.org/10.1016/j.gexplo.2016.04.007.

Zanobetti, A., Gold, D.R., Stone, P.H., Suh, H.H., Schwartz, J., Coull, B.A., Speizer, F.E., 2010. Reduction in heart rate variability with traffic and air pollution in patients with coronary artery disease. Environ. Health Perspect. 118 (3), 324-330.

Zhang, J., Peng, J., Song, C., Ma, C., Men, Z., Wu, J., Wu, L., Wang, T., Zhang, X., Tao, S., Gao, S., Hopke, P.K., Mao, H., 2020. Vehicular non-exhaust particulate emissions in Chinese megacities: source profiles, real-world emission factors, and inventories. Environ. Pollut. 266 https://doi.org/10.1016/j.envpol.2020.115268.

Zhao, W., Hopke, P.K., Gelfand, E.W., Rabinovitch, N., 2007. Use of an expanded receptor model for personal exposure analysis in schoolchildren with asthma. Atmos. Environ. 41, 4084-4096. https://doi.org/https://doi.org/10.1016/j.atmosenv.2007.01.037

Supplementary information

PMF model runs

The input data for PMF included a 24 x 90 and a 21 x 90 (samples x species) matrix for coarse and fine PM respectively. One hundred model runs were performed, and the convergent solution with the lowest Q/Qexp value was selected. Qrobust values were also compared to Qtrue values to examine the impact of outliers. Residuals were inspected for normality and solution stability. Inspection of Q values indicated no undue influence from outliers and no local minima in all size fractions. The range in Q values was evaluated confirm that selected solutions were a global rather than local minimum. The Q/Qexp values represented the ratios between the actual sum of the squares of the scaled residuals (Q) obtained from the PMF least squares fit and the ideal Q (Qexp), which was obtained if the fit residuals at each point were equal to the noise specified for each data point. Nine different modelling conditions were examined with number of factors ranging from 3 to 10 where each simulation was randomly conducted 100 times. The optimum solution for coarse and fine PM, as suggested by the Q/Qexp ratio, is shown in Figure S2.

A signal to noise condition was additionally applied in the data. Individual species that retained a significant signal were separated from those dominated by noise. When signal to noise (S/N) ratio was < 0.2, species were judged as bad and removed from the analysis. Species with 0.2 < S/N < 2 were characterized as weak and their uncertainty was tripled. Species with S/N ratio greater than 2 (S/N > 2) were defined as strong and remained unchanged.

Base Solution, Rotations and Uncertainty Evaluations

Uncertainty in the PMF solution was examined using bootstrapping to evaluate the effect of random errors. G space plots were also evaluated for rotational ambiguity and correlations between factor contributions. Based on bootstrapping results and G space plots inspection, Fpeak rotations were attempted, with positive F peak values to sharpen the F matrix and negative values to sharpen the G matrix. The optimal Fpeak value for solution rotation was chosen based on the smallest change in Q, interpretability of profiles, improvement in bootstrap results, and fewer edges in G space plots when expected. One hundred bootstrap runs were attempted with a minimum correlation of 0.6. Fpeak values of +0.5 resulted in optimal rotated solutions with smallest dQ values, decreased bootstrap factor swapping and reduced G space plot edges in the rotated versus base solution, for coarse and fine PM fractions, respectively.

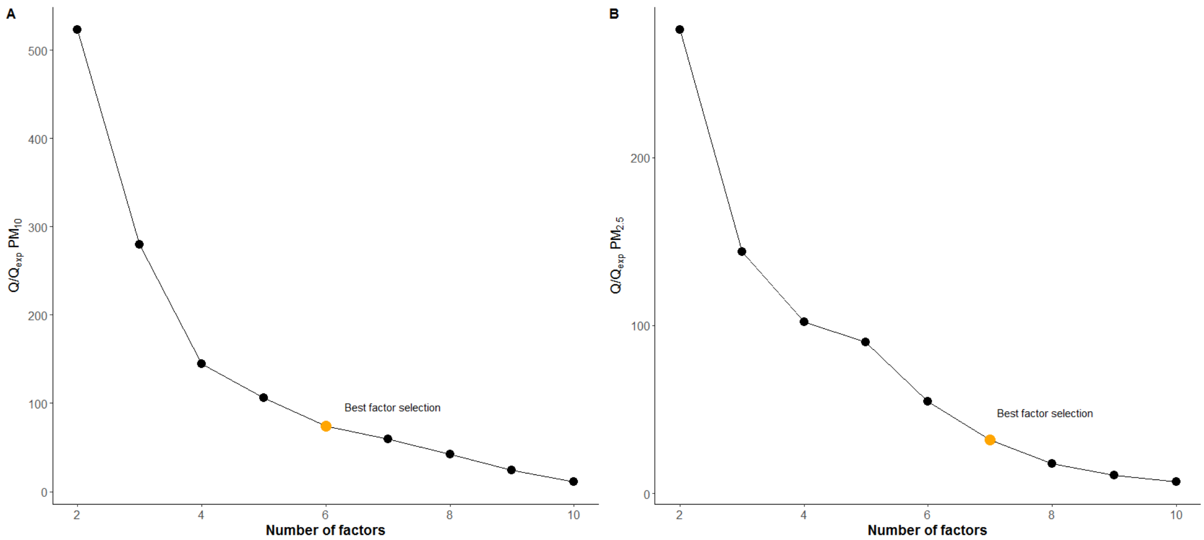

Figure S1. PMF diagnostic Q/Qexpected plot. Q = the sum of squared scaled residuals over the whole dataset, plotted versus the number of factors used in the PMF solution. Orange circle indicates the optimum solution.

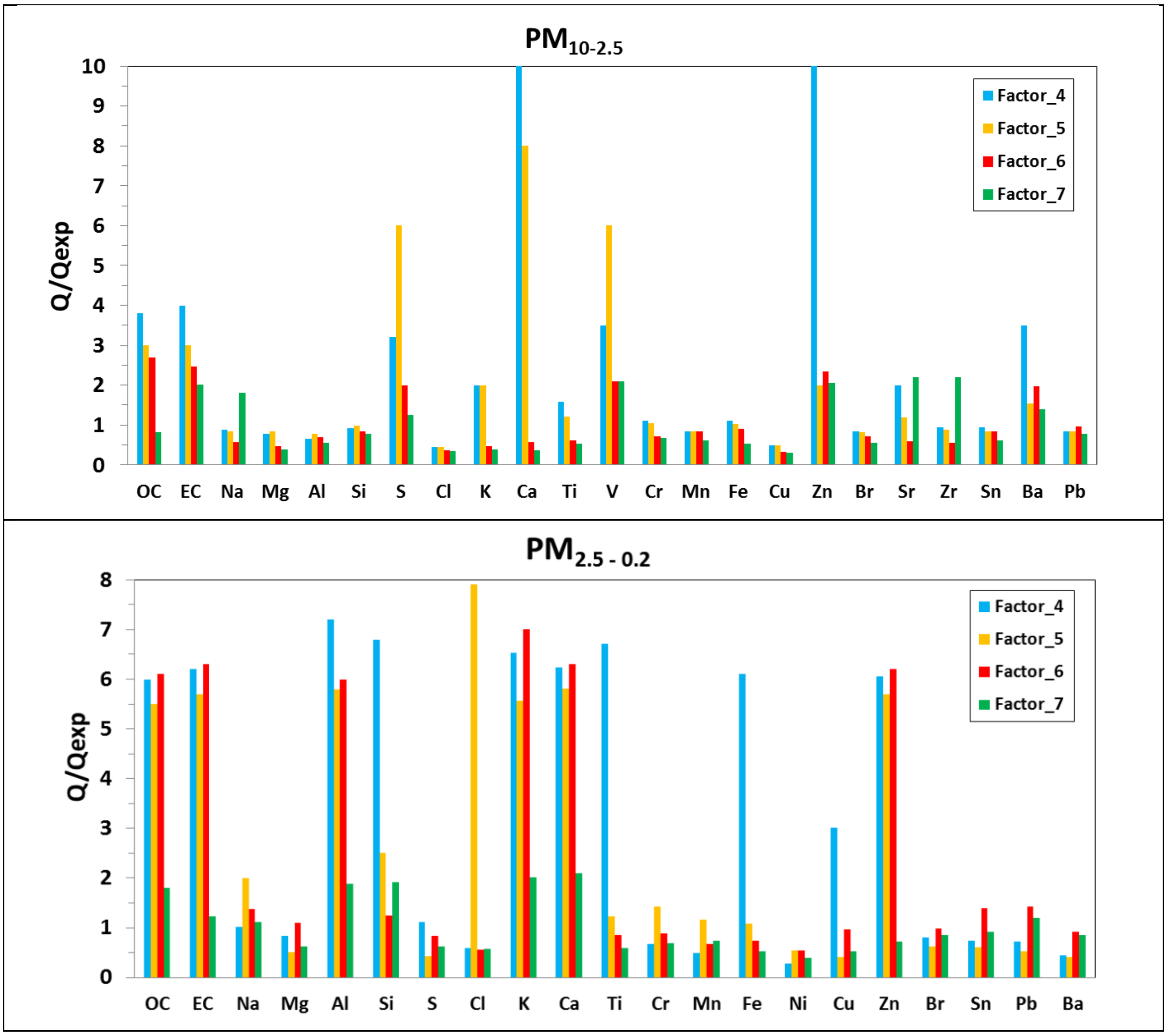

Figure S2. Species Q/Qexpected for 4 to 7 factor solution for $PM_{10-2.5}$ and $PM_{2.5-0.2}$.

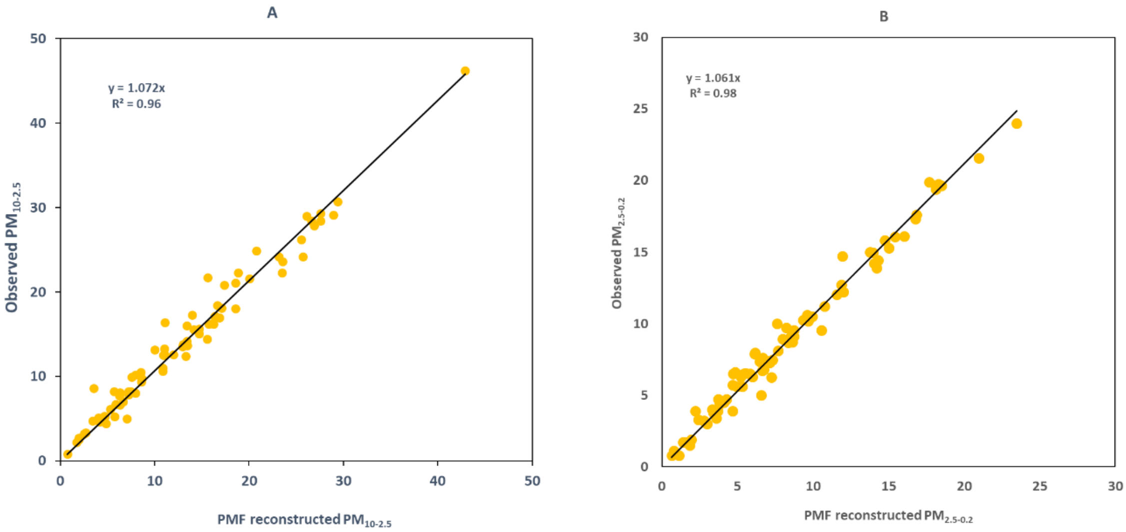

Figure S3. Observed and PMF predicted coarse (A) and fine (B) PM. The solid line shows the 1:1 ratio.

Figure S4 $PM_{10-2.5}$ PMF source contributions at different road distances

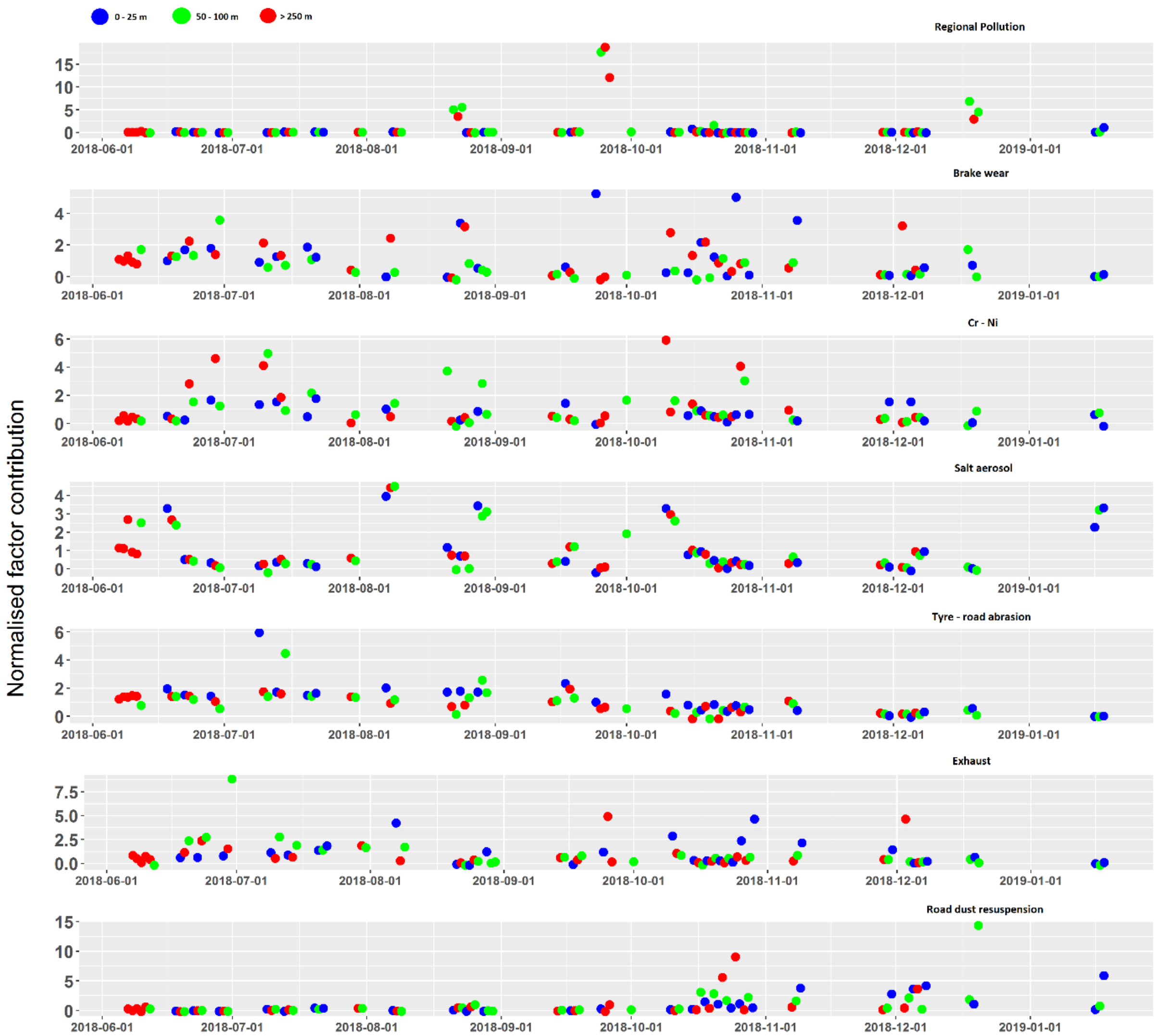

Figure S5 $PM_{2.5-0.2}$ PMF source contributions at different road distances

Table S1. $PM_{10-2.5}$ PMF diagnostics output

$PM_{10-2.5}$ BS-DISP Diagnostics:

# of Cases Accepted: 94

% of Cases Accepted: 94%

Largest Decrease in Q: -7.457

%dQ: -0.5181

# of Decreases in Q: 0

# of Swaps in Best Fit: 0

# of Swaps in DISP: 9

Swaps by Factor: 0 0 0 4 0 3

$PM_{10-2.5}$ DISP Diagnostics:

Error Code: 0

Largest Decrease in Q: -0.01

%dQ: -0.00023

Swaps by Factor: 0 0 0 0 0 0

$PM_{10-2.5}$ BS Mapping:

	Salt	Road dust	Tyre-Road abrasion	Regional pollution	Exhaust	Brake wear	Unmapped
Boot Salt	99	1	0	0	0	0	0
Boot Road dust	0	95	4	0	0	1	0
Boot Tyre-Road abrasion	0	2	95	0	1	2	0
Boot Regional pollution	0	0	0	97	2	1	0
Boot Exhaust	0	0	0	0	100	0	0
Boot Brake wear	0	0	0	0	0	100	0

Table S2. $PM_{2.5-0.2}$ PMF diagnostics output

$PM_{2.5-0.2}$ BS-DISP Diagnostics:

# of Cases Accepted: 91

% of Cases Accepted: 91%

Largest Decrease in Q: -4.544

%dQ: -0.094791

# of Decreases in Q: 0

# of Swaps in Best Fit: 0

# of Swaps in DISP: 8

Swaps by Factor: 2 0 0 0 0 4 0

$PM_{2.5-0.2}$ DISP Diagnostics:

Error Code: 0

Largest Decrease in Q: -0.191

%dQ: -0.00202

Swaps by Factor: 0 0 0 0 0 0 0

$PM_{2.5-0.2}$ BS Mapping:

	Regional pollution	Brake wear	Cr-Ni	Salt	Tyre-Road abrasion	Exhaust	Road dust resuspension	Unmapped
Boot Regional pollution	100	0	0	0	0	0	0	0
Boot Brake wear	0	100	0	0	0	0	0	0
Boot Cr-Ni	0	0	100	0	0	0	0	0
Boot Salt	0	0	0	99	1	0	0	0
Boot Tyre-Road abrasion	0	0	0	0	100	0	0	0
Boot Exhaust	0	0	0	0	0	99	1	0
Boot Road dust resuspension	0	0	0	0	0	0	100	0

Table S3. Mean $PM_{10-2.5}$ and $PM_{2.5-0.2}$ mass and elemental composition

	Coarse		Fine	
Element	Mean (ng/m^3)	SD (ng/m^3)	Mean (ng/m^3)	SD (ng/m^3)
PM	6,140	4,420	8,880	5,450
OC	649	427	2243	1241
EC	113	65.8	552	481
Na	89.5	179	91.4	153
Mg	30.3	29.2	34.1	33.2
Al	162	149	186	169
Si	372	359	171	207
S	33.2	25.8	373	365
Cl	156	417	83.3	242
K	65.6	56	56.2	44.1
Ca	152	201	76.4	15.6
Ti	18.3	22	13.3	12.4
V	0.58	0.74	-	-
Cr	0.58	0.71	11.0	19.5
Mn	3.6	3.1	4.4	4.0
Fe	221	213	204	193
Cu	6.1	9.8	9.2	7.9
Zn	5.61	5.5	27.8	24.1
Br	0.61	0.38	2.71	2.13
Sr	1.29	1.33	-	-
Zr	2.89	4.9	-	-
Sn	1.87	2.1	6.83	7.3
Ba	13.7	23.8	-	-
Pb	1.22	0.89	5.23	4.6
Ni	-	-	3.97	7.61

Brake Wear SGAM results

```
Family: gaussian
Link function: log

Formula:
(brake.wear.pm10) ~ count + time + temp

Parametric coefficients:
            Estimate Std. Error t value Pr(>|t|)
(Intercept)  2.091e+01  2.925e+00   7.148 4.89e-10 ***
count        5.848e-04  2.254e-04   2.595   0.0114 *
time        -3.111e-01  5.591e-02  -5.564 3.89e-07 ***
temp         1.839e-01  2.281e-02   8.062 9.08e-12 ***
---
Signif. codes:  0 '***' 0.001 '**' 0.01 '*' 0.05 '.' 0.1 ' ' 1


R-sq.(adj) =  0.814   Deviance explained = 76.2%
-REML = 125.44  Scale est. = 1.0081    n = 89
```

```
Family: gaussian
Link function: log

Formula:
(brake.wear.pm2.5) ~ s(temp, k = 2) + rh + s(Distance..m., k = 4) + count

Parametric coefficients:
            Estimate Std. Error t value Pr(>|t|)
(Intercept) -1.451e+00  1.630e+00  -0.890   0.3762
rh          -3.589e-02  1.598e-02  -2.246   0.0276 *
count        1.366e-04  2.439e-05  -0.560   0.0370 *
---
Signif. codes:  0 '***' 0.001 '**' 0.01 '*' 0.05 '.' 0.1 ' ' 1

Approximate significance of smooth terms:
                  edf Ref.df     F p-value
s(temp)         1.470      2 2.190 0.05721 .
s(Distance..m.) 1.803      3 4.541 0.00107 **
---
Signif. codes:  0 '***' 0.001 '**' 0.01 '*' 0.05 '.' 0.1 ' ' 1

R-sq.(adj) =  0.232   Deviance explained = 27.4%
-REML = 164.91  Scale est. = 1.9245    n = 88
```

Exhaust SGAM results

```
Family: gaussian
Link function: log

Formula:
(exhaust.pm10) ~ Road.ID + lanes + s(t, k = 5) + s(time, k = 3)

Parametric coefficients:
          Estimate Std. Error t value Pr(>|t|)
(Intercept) -1.88946    0.70902  -2.665  0.00949 **
Road.ID       0.38266    0.18100   2.114  0.03794 *
lanes          0.20764    0.06767   3.068  0.00302 **
---
Signif. codes:  0 ‘***’ 0.001 ‘**’ 0.01 ‘*’ 0.05 ‘.’ 0.1 ‘ ’ 1

Approximate significance of smooth terms:
        edf Ref.df     F  p-value
s(temp) 1.727      4 6.771 2.66e-06 ***
s(time) 1.711      2 7.744 0.000308 ***
---
Signif. codes:  0 ‘***’ 0.001 ‘**’ 0.01 ‘*’ 0.05 ‘.’ 0.1 ‘ ’ 1

R-sq.(adj) =  0.436   Deviance explained = 47.5%
-REML = 80.925  Scale est. = 0.36803   n = 89
```

```
Family: gaussian
Link function: log

Formula:
(exhaust.pm2.5) ~ temp + time + count

Parametric coefficients:
            Estimate Std. Error t value Pr(>|t|)
(Intercept) -1.557e+00  7.324e-01  -2.126 0.036642 *
temp       -2.341e-02  6.282e-03   3.726 0.000364 ***
time        -1.759e-01  1.076e-01  -0.163 0.087055 .
count       6.012e-04  1.499e-04   0.401 0.068947 .
---
Signif. codes:  0 ‘***’ 0.001 ‘**’ 0.01 ‘*’ 0.05 ‘.’ 0.1 ‘ ’ 1


R-sq.(adj) =  0.205   Deviance explained = 23.4%
-REML = 120.38  Scale est. = 0.73744   n = 88
```

Road dust resuspension SGAM results

```
Family: gaussian
Link function: log

Formula:
(road.dust.resuspension.pm10) ~ speed.limit + s(temp, k = 4) + s(rh, k = 3) + s(ws, k = 5) + time

Parametric coefficients:
            Estimate Std. Error t value Pr(>|t|)
(Intercept)  2.50512    0.62693   2.401 0.019032 *
speed.limit  0.04141    0.01066  -3.884 0.000231 ***
time        -0.25115    0.13559   1.968 0.052988 .
---
Signif. codes:  0 ‘***’ 0.001 ‘**’ 0.01 ‘*’ 0.05 ‘.’ 0.1 ‘ ’ 1

Approximate significance of smooth terms:
          edf Ref.df      F  p-value
s(temp) 1.887      3  6.281 7.52e-05 ***
s(rh)   1.651      2  3.672   0.0144 *
s(ws)   2.725      4 19.756  < 2e-16 ***
---
Signif. codes:  0 ‘***’ 0.001 ‘**’ 0.01 ‘*’ 0.05 ‘.’ 0.1 ‘ ’ 1

R-sq.(adj) =  0.745   Deviance explained =   77%
-REML = 151.89  Scale est. = 1.8428    n = 89
```

```
Family: gaussian
Link function: log

Formula:
(road.dust.resuspension.pm2.5) ~ temp + time + rh + ws

Parametric coefficients:
             Estimate Std. Error t value Pr(>|t|)
(Intercept)  3.339792   1.261006   2.649  0.00978 **
temp         0.004492   0.003246   0.620  0.05370 .
time        -0.912078   0.330921  -2.137  0.03576 *
rh          -0.031050   0.014453  -2.148  0.03479 *
ws           0.178904   0.079159  -0.226  0.00180 **
---
Signif. codes:  0 ‘***’ 0.001 ‘**’ 0.01 ‘*’ 0.05 ‘.’ 0.1 ‘ ’ 1


R-sq.(adj) =  0.113   Deviance explained = 13.6%
-REML = 145.42  Scale est. = 1.6732    n = 88
```

Tyre – Road abrasion SGAM results

```
Family: gaussian
Link function: log

Formula:
(road.tyre) ~ Distance..m. + count + s(speed.limit, k = 5) + temp + time

Parametric coefficients:
            Estimate Std. Error t value Pr(>|t|)
(Intercept)  -5.915e+00  1.230e+00  -4.810 8.35e-06 ***
Distance..m. -1.540e-02  2.434e-03  -6.327 2.04e-08 ***
count        1.163e-04  2.153e-05   5.401 8.58e-07 ***
temp         6.642e-02  1.984e-02   3.348  0.00131 **
time        -0.658e+00  0.184e+00   5.207 1.83e-06 ***
---
Signif. codes:  0 ‘***’ 0.001 ‘**’ 0.01 ‘*’ 0.05 ‘.’ 0.1 ‘ ’ 1

Approximate significance of smooth terms:
              edf Ref.df     F  p-value
s(speed.limit) 3.873      4 9.549 2.68e-06 ***
---
Signif. codes:  0 ‘***’ 0.001 ‘**’ 0.01 ‘*’ 0.05 ‘.’ 0.1 ‘ ’ 1

R-sq.(adj) =  0.842   Deviance explained = 81.6%
-REML = 130.75  Scale est. = 0.73573   n = 89
```

```
Family: gaussian
Link function: log

Formula:
road.tyre ~ s(temp, k = 5) + time + count

Parametric coefficients:
            Estimate Std. Error t value Pr(>|t|)
(Intercept)  1.960e+02  8.060e+02   2.243    0.808
time       -7.197e-02  2.225e-03  -1.323    0.0747 .
count       2.134e-04  1.109e-04   1.246    0.0806 .

Approximate significance of smooth terms:
       edf Ref.df     F p-value
s(temp) 1.835      3 1.943  0.0475 *
---
Signif. codes:  0 ‘***’ 0.001 ‘**’ 0.01 ‘*’ 0.05 ‘.’ 0.1 ‘ ’ 1

R-sq.(adj) =  0.855   Deviance explained = 83.7%
-REML = 120.12  Scale est. = 0.8222    n = 88
```